BACHELOR

Computation of charge mobility in a disordered polymer system by solving the master equation

Cottaar, J.

Award date:
2005

Computation of Charge Mobility in a Disordered Polymer System by Solving the Master Equation

Jeroen Cottaar

10th June 2005

Contents

Chapter 1

Introduction

1.1 Formalities

This project was done as a required internship for the physics and mathematics study at the University of Technology in Eindhoven. My coaches were Peter Bobbert(physics) at Polymer Physics and Frank Redig(mathematics) at Stochastics and Decision Analysis. I worked on this from April 2004 to June 2005, although only very part time from July 2004 to April 2005.

1.2 Problem background

Since the 1970s there has been extensive research into the conducting properties of conjugated polymers. Although at first the focus was on achieving metallic conductivity by using high doping, in the past years the focus has shifted to the semiconducting properties observed with little or no doping.
Polymer-based logic circuits have some large advantages over tradition silicon-based circuits[1]. In the first place they can be processed at relative low temperatures, of the order of 200 degrees Celsius, leading to significantly lower production costs. Also, the components keep their semiconducting properties when deformed, i.e. a polymer chip can be bent without impeding functionality. However, their is also a large disadvantage: the carrier mobility is still significantly lower than in silicon-based semiconductors, and so the switch frequency will never approach those of traditional components.
It is even possible to make electroluminescent devices such as LEDs and LCDs[2]. These are two-carrier devices which generate light by the recombination of holes and electrons. Although only single-carrier devices will be considered here, two-carrier device characteristics can be calculated once both carrier mobilities are known.
To calculate performance characteristics of these devices it is important to know the charge mobility as a function of the electric field, the temperature and the

amount of doping, i.e. the carrier density. Although the field and temperature dependence has been extensively studied[3, 4, 5, 6], these were unable to fully explain device characteristics without extra assumptions. However, these did not take into account that a higher voltage over the device increases not only the electric field but also the carrier density. To fully understand these devices we therefore need a unified theoretical description of the mobility dependence on all three factors listed[7]. This then is the problem that will be tackled here.

1.3 General approach

The generally accepted model for polymer conductance is that there are conjugated polymer chain segments which allow a localized electron wave function. These segments are referred to as sites. The energy levels for these wave functions are site dependent and follow a Gaussian distribution. This distribution has in fact been approximately confirmed by recent experiments[8].
An electron can tunnel from one site to another with a certain jump rate. This process is called hopping, and for the rate at which it occurs the Miller-Abrahams rate is used[9]. The field is taken into account by adding a field-assisted term to the energy difference between sites. Doping is also important because no two electrons can occupy one site due to Coulomb repulsion.
What we will now do is calculate or approach the distribution of charge carriers over the sites, and calculate the mobility from this distribution. Once the mobility is known as a function of field, carrier concentration and temperature, device characteristics can be computed.

1.4 Report structure

Chapter 2 will discuss the theory behind our solution. First, the model used will be described fully(2.1), followed by a dimensional analysis(2.2). We will then consider ways to describe the distribution or approximate distribution of electrons in the polymer(2.3). Then the way to calculate the mobility from this distribution will be described(2.4). The zero-field case(2.5) and a way to visualize the effect of the field on the distribution using the electrochemical potential(2.6) will then be discussed. The chapter on theory will conclude with a description of the application to single-carrier devices(2.7).
After this, in chapter 3, the implementation, i.e. ways to actually calculate the approximate charge carrier distributions, will be discussed. First the general iteration scheme will be presented(3.1), followed by some details of the implementation(3.2).
After that the results will be presented in chapter 4. First the main results of the project, field(4.1), density and temperature dependence(4.2) of the mobility will be shown. After that the validity of the approximation of the distribution,

essentially a mean-field approach, will be demonstrated(4.3). Also, it will be shown that it is necessary to take the influence of the field on the distribution into account(4.4). Finally, the graphs of the electrochemical potential(4.5) and results for single-carrier devices(4.6) will be presented.
Finally, the conclusions of this project will be discussed in chapter 5.

Chapter 2

Theory

2.1 Model

We imagine the polymer as an infinite cubic lattice of sites. Any site may be occupied by an electron or not; there can never be more than one. The distance between two sites in this lattice will be referred to as R_0. To make calculations possible the lattice is limited to a cube of L sites in length, with periodic boundary conditions. Of course, for results to be valid we must consider the limit where L tends to infinity.
Now, an electron occupying a site will possess a certain energy. This energy is a property of the site in question and will be referred to as ϵ_i. The index i identifies the site being considered. The ϵ_i are taken from some random distribution; in the remainder of this report they are considered independent and normally distributed with mean 0 and variance σ^2, where σ is a measure for the disorder of the system.
To have mobility we need conduction, i.e. a way for the electrons to move. An electron occupying site i can tunnel to some unoccupied site j. The rate at which these jumps occur will be written as W_{ij} and is the product of three factors. The first is simply a constant, ν_0. The second factor is determined by the overlap of the electron wave functions at the sites, causing it to depend exponentially on the distance between them. It is given by $\exp(-\alpha|\vec{r_j} - \vec{r_i}|)$. Here, α is a constant, the inverse localization length, and $\vec{r_i}$ and $\vec{r_j}$ are the locations of the sites.
The third factor is determined by the energy difference $\Delta\epsilon$ between the two sites. Without an electric field this is simply $\epsilon_j - \epsilon_i$. However, we can only have mobility with a field. Taking it into account, the energy difference becomes $\epsilon_j - \epsilon_i - e\vec{E} \cdot (\vec{r_j} - \vec{r_i})$. Here, e is the charge of an electron and $\vec{E}$ the electric field. Note that we cannot take the field into account by simply subtracting $e\vec{E} \cdot \vec{r_i}$ from each ϵ_i since we are using periodic boundary conditions.
Now, an electron jumping to a site with a lower energy(as given by $\Delta\epsilon$ above) will not be hindered by this energy difference. To reach a site with a higher en-

ergy, the electron will need thermal fluctuations. This yields a Boltzmann term $\exp(-\Delta\epsilon/kT)$ with k Boltzmann's constant and T the temperature, applicable only when $\Delta\epsilon \geq 0$.
Combining all of this yields the following equation for the jump rates:

$$W_{ij} = \begin{cases} \nu_0 \exp(-\alpha * |\vec{r_j} - \vec{r_i}|) \exp(-(\epsilon_j - \epsilon_i - e\vec{E} \cdot (\vec{r_j} - \vec{r_i}))/kT) \\ \text{if } (\epsilon_j - \epsilon_i - e\vec{E} \cdot (\vec{r_j} - \vec{r_i})) \geq 0 \\ \nu_0 \exp(-\alpha * |\vec{r_j} - \vec{r_i}|) \\ \text{if } (\epsilon_j - \epsilon_i - e\vec{E} \cdot (\vec{r_j} - \vec{r_i})) \leq 0 \end{cases} \tag{2.1}$$

Keep in mind that this jump rate only applies to an occupied site i and an unoccupied site j; otherwise no jumps are possible.
Note that, due to the periodic boundary conditions, $\vec{r_i}$ and $\vec{r_j}$ are not uniquely defined. They should be chosen so that the distance $|\vec{r_j} - \vec{r_i}|$ is minimal.
There are two important parameters that still need to be defined. These are the electron density per site n and the charge mobility μ. The electron density per site n is defined as the asymptotic (in time) probability that a randomly chosen site is occupied. In the case of our finite lattice with periodic boundary conditions this simplifies to the number of electrons divided by the number of sites, L^3. The charge mobility is defined as the average velocity of an electron in the direction of the electric field divided by the size of the field.

2.2 Dimensional analysis

In section 2.1 all parameters relevant to the model were introduced. These are summarized in table 2.2.

This is quite a list of parameters, each of which(except for the constants of

Symbol	Description	Unit
α	Tunneling rate	m^{-1}
T	Thermal energy	J
E	Electric field	V/m
n	Electron density	1
σ	Energy spread	J
ν_0	Jump rate prefactor	s^{-1}
R_0	Distance between sites	m
L	Size of the sample considered	1
e	Electron charge	C
k	Boltmann's constant	J/K

Table 2.1: List of parameters in our model. A full description of these parameters can be found in section 2.1.

course) can influence the charge mobility. However, we can decrease the size of

this list considerably. In the first place, we always consider the limit of large L, so it can be removed. Furthermore, k and T only occur as each other's product. Taking this into account and rewriting the remaining parameters yields the list shown in table 2.2.

Simple dimensional analysis now tells us that the charge mobility depends on

Parameter	Unit
ν_0	s^{-1}
R_0	m
e	C
σ	J
eER_0/σ	1
σ/kT	1
n	1
αR_0	1

Table 2.2: Reduced list of parameters in our model.

these parameters as:

$$\mu = f(eER_0/\sigma, \sigma/kT, n, \alpha R_0)\frac{R_0^2\nu_0 e}{\sigma} \tag{2.2}$$

From now on the respective arguments of the function f will be referred to as the dimensionless field, inverse temperature, density and inverse localization length. The value of the function itself will be referred to as the dimensionless mobility.

2.3 Balance equations

2.3.1 Definitions

In this section a set of equations will be derived to approximately describe the distribution of charge carriers.

First, let us consider the general method of finding the distribution in this model. We define a configuration of the system as a full description of its state. Let η be such a configuration. It can be represented as a list of bits, each one representing an empty site or one occupied by an electron. $\eta_i = 0, 1$ describes whether site i is occupied. Finally, use Π to refer to the set of all possible configurations.

A distribution on the system is some probability measure on Π. If ζ is such a distribution, we write $\zeta(\eta)$ for the probability that the system is in some state η. If f is some real function on Π, we define its expectation value $< f >_\zeta$ using the familiar equation:

$$< f >_\zeta = \sum_{\eta \in \Pi} f(\eta)\zeta(\eta) \tag{2.3}$$

The dynamics of the system can be formalized using the infinitesimal generator G_t. This operator maps sufficiently smooth functions on Π onto this same set of functions and is defined by:

$$< G_t f >_\zeta = \frac{d}{dt} < f >_\zeta \tag{2.4}$$

which must hold for all functions f and distributions ζ.
Now let us try to find this generator explicitly for our system. Write $\eta_{i \leftrightarrow j}$ for configuration η with the occupation numbers of sites i and j switched. If the system is in some configuration η with site i occupied, it will change to $\eta_{i \leftrightarrow j}$ with rate W_{ij}(as defined in equation 2.1), for all i and j. Note that the condition that site j is empty is implicit in this, since otherwise $\eta_i = \eta_j = 1$ and so $\eta_{i \leftrightarrow j} = \eta$. We now have:

$$(G_t f)(\eta) = \sum_{i,j} W_{ij}(f(\eta_{i \leftrightarrow j}) - f(\eta))\eta_i \tag{2.5}$$

Finally, we need to define a limiting distribution in terms of the infinitesimal generator. A limiting distribution α is defined as one to which the system can converge in time. In other words, all expectation values of functions on Π must be constant for this distribution, leading to the condition(using equation 2.4):

$$< G_t f >_\alpha = 0 \tag{2.6}$$

for all functions f. More on this can be found in [10].
We can now proceed to derive the equations to describe such a limiting distribution. Its existence and uniqueness must of course also be shown.

2.3.2 Full balance equations

Consider a limiting distribution α and some configuration η. Define the function f_η on Π by $f_\eta(\eta) = 1$ and $f_\eta(x) = 0$ for $x \neq \eta$. Evaluating the result of applying G_t to this function will yield the formulas describing α. Using equation 2.5, we find:

$$\begin{aligned}
&(G_t f_\eta)(\eta) = \sum_{i,j} W_{ij}(f_\eta(\eta_{i \leftrightarrow j}) - f_\eta(\eta))\eta_i = -\sum_{i,j} W_{ij}\eta_i(1 - \eta_j) \\
&(G_t f_\eta)(x) = \sum_{i,j} W_{ij}(f_\eta(x_{i \leftrightarrow j}) - f_\eta(x))x_i = W_{ji}\eta_i(1 - \eta_j),\ x = \eta_{i \leftrightarrow j} \\
&(G_t f_\eta)(x) = 0,\ \text{otherwise}
\end{aligned} \tag{2.7}$$

Now, α is a limiting distribution, so we may apply equation 2.6 to find:

$$0 =< G_t f_\eta >_\alpha = \sum_x (G_t f_\eta)(x)\alpha(x) = \sum_{i,j} (W_{ij}\eta_i(1-\eta_j)\alpha(\eta) - W_{ji}\eta_i(1-\eta_j)\alpha(\eta_{i\leftrightarrow j})) \tag{2.8}$$

When applied to every configuration η this yields a set of equations which, combined with the normalization condition, can be used to determine α.
This result would also have been found by considering our model as a finite-state continuous Markov process. The above method was used because it will allow the simplifications applied later on to be explained more clearly. However, for existence and uniqueness we will simply use results from Markov theory. These state that the limiting distribution exists and is unique if the process is ergodic, i.e. every configuration must be reachable(not necessarily directly) from every other one. This last condition is satisfied in our case if we fix the number of electrons by specifying the electron density n.
Unfortunately, for typical sample sizes like 50x50x50, there are 2^{125000} possible configurations. This means that actually solving equation 2.8 is impractical; instead we should concentrate on finding distributions that approach α.

2.3.3 Approaching the limiting distribution

A standard approach now is to assume that the occupation of a site is independent of the occupation of any other site, a mean-field approximation. Here, we consider a more general approach, where we take clusters of sites and assume them to be independent of each other.
First, some definitions. Let X be any partitioning of all sites, and take $x \in X$. Let Π_x be the set of all possible configurations of the cluster of sites x. If η is a configuration of the whole system, then let η_x be the configuration of the cluster x. Define the function $f_{x,g}$ for $x \in X$ and $g \in \Pi_x$ by $f_{x,g}(\eta) = 1$ if $\eta_x = g$ and $f_{x,g} = 0$ otherwise. For $i \in x$ let g_i be the number of electrons at site i in configuration g, 0 or 1. Finally, let N_g be the total number of electrons in x in configuration g.
Consider a distribution ζ. It is called a product distribution over X if it satisfies:

$$\zeta(\eta) = \prod_{y \in X} < f_{y,\eta_y} >_\zeta \tag{2.9}$$

Define $\zeta_{x,g}$ by $\zeta_{x,g} =< f_{x,g} >_\zeta$. These numbers specify ζ if it is a product distribution.
We now want to find a product distribution α over X that is close to the limiting distribution. Of course, we can't expect it to satisfy equation 2.6 completely. Instead, we want it to satisfy:

$$< G_t f_{x,g} >_\alpha = 0 \tag{2.10}$$

for all $x \in X$ and $g \in \Pi_x$. This set of equations is not yet sufficient to fully determine $\alpha_{\cdot,\cdot}$. We also need the following(trivial) conditions:

$$\sum_{h \in \Pi_x} \alpha_{x,h} = 1 \tag{2.11}$$

$$0 \leq \alpha_{x,g} \leq 1 \tag{2.12}$$

again for all $x \in X$ and $g \in \Pi_x$.
Finally, we need to set the number of electrons in the system. Note that it is impossible for non-trivial product distributions to have this constant. Instead, we want its expectation value to match the condition set by the electron density, yielding:

$$\sum_{y \in X} \sum_{h \in \Pi_y} N_h \alpha_{x,h} = nL^3 \tag{2.13}$$

We will find that this set of equations(2.10 through 2.13) is sufficient to describe α. They can be considerably worked out for the general case, but we will leave them in this form for now and work them out fully only for the case of partitioning into clusters of one or two sites each.

2.3.4 Clusters of one or two sites

Let the partitioning X consist of partitions of one element each. So, we are now simply considering each site to be independent from all other sites. We are looking for the product distribution over X α satisfying equations 2.10 through 2.13. Following standard notation, we write $p_g = \alpha_{\{g\},\{1\}}$, and so, by equation 2.11, $\alpha_{\{g\},\{0\}} = 1 - p_g$. Furthermore, let $f_g = f_{\{g\},\{1\}}$, so $f_g(\eta) = \eta_g$. We have, using equation 2.5:

$$(G_t f_g)(\eta) = \sum_{i,j} W_{ij}(f_g(\eta_{i \leftrightarrow j}) - f_g(\eta))\eta_i = \sum_i (W_{ig}\eta_i(1-\eta_g) - W_{gi}\eta_g(1-\eta_i)) \tag{2.14}$$

Now, using equation 2.10:

$$\begin{aligned} 0 =& < G_t f_g >_\alpha = \sum_{\eta \in \Pi} (G_t f_g)(\eta)\alpha(\eta) = \\ & \sum_{\eta \in \Pi} \sum_i ((W_{ig}\eta_i(1-\eta_g) - W_{gi}\eta_g(1-\eta_i)) \prod_j (\eta_j p_j + (1-\eta_j)(1-p_j))) = \\ & \sum_i (W_{ig}p_i(1-p_g) - W_{gi}p_g(1-p_i)) \end{aligned} \tag{2.15}$$

Multiplying by -1, renaming indices and including equations 2.12 and 2.13 yields a very familiar set of equations:

$$\begin{array}{l} \sum_j (W_{ij} p_i (1-p_j) - W_{ji} p_j (1-p_i)) = 0 \\ 0 \leq p_i \leq 1 \\ \sum_j p_j = nL^3 \end{array} \tag{2.16}$$

This is of course the well known Master equation, and it is the one we will mostly be solving. However, we must still check whether this one-site simplification is justified; to do this we consider clusters of two sites. If the results do not differ greatly then we can expect them to be approximately equal to those obtained by solving the full balance equation 2.8. How to derive the equivalent of equation 2.16 for the case of two-site clusters is shown in appendix A.

2.4 Calculating charge mobility

We have been discussing the limiting distribution for some time, but it is generally not this distribution we want to know; we are interested in the charge mobility in this distribution. So, let's examine how we can evaluate it, working from the definition given in section 2.1. First, let's calculate the total velocity of all electrons in some distribution α, not yet taking into account periodic boundary conditions:

$$\begin{array}{l} (\vec{v}_T)_\alpha = \frac{d}{dt} < \vec{r}_T >_\alpha = < G_t \vec{r}_T >_\alpha \\ \vec{r}_T(\eta) = \sum_i \eta_i \vec{r}_i \end{array} \tag{2.17}$$

Note that $\vec{v_T}$ is necessarily equal to 0 if α is a product distribution by equation 2.9. However, this is only because we haven't taken periodic boundary conditions into account yet. Writing out equation 2.17 using equation 2.5 yields:

$$(\vec{v}_T)_\alpha = \sum_{\eta,i,j} \alpha(\eta) W_{ij} \eta_i (1-\eta_j)(\vec{r}_j - \vec{r}_i) \tag{2.18}$$

Periodic boundary conditions can now be taken into account by choosing $\vec{r}_j$ and $\vec{r}_i$ in the same way as for equation 2.1, i.e. by taking them so that $|\vec{r}_j - \vec{r}_i|$ is minimal. To calculate the mobility from this, we assume that the current is in the direction of the field. We must divide by the field and the number of electrons. This yields, for the one-site cluster case(using the notation of section 2.3.4):

$$\mu = \frac{\sum_{i,j} W_{ij} p_i (1-p_j)(\vec{r}_j - \vec{r}_i) \cdot \hat{E}}{nL^3 |\vec{E}|} \tag{2.19}$$

The equivalent of equation 2.19 for the case of two-site clusters can be found in appendix A.

2.5 The zero-field case

Consider one-site clusters with $\vec{E} = 0$. Fermi statistics apply and we have:

$$p_i = \frac{1}{\exp((\epsilon_i - \epsilon_F)/kT) + 1} \tag{2.20}$$

where ϵ_F is the Fermi level, which should be chosen so that the third part of equation 2.16, the density condition, is satisfied. Note that the first two parts of this equation are also satisfied, as was to be expected.
Using equation 2.19 without dividing by the field, it can easily be checked that the current evaluates to 0 for this distribution(each term is cancelled out by the one in which i and j are interchanged), i.e. there is no current in the zero-field case. This too was of course to be expected.
There is one less trivial characteristic of the zero-field case: it satisfies equation 2.8, i.e. the one-site product distribution is completely accurate in this case. Unfortunately, this result does not hold when a field is applied, as we will find later.
Note that instead of solving equation 2.16 to approximate the limiting distribution we could also take the distribution specified by equation 2.20 above, i.e. pretend the field is not there. We then use the actual jump rates, taking the field into account, in equation 2.19 to find the mobility. This approach was used by Roichman and Tessler[11]; we will see later that this approximation, although computationally efficient, is too crude.

2.6 The electrochemical potential

In the case of one-site clusters, there is a nice way to visualize the influence of the electric field on the movement of the electrons. This is done using the electrochemical potential μ_i, defined for every site i by:

$$p_i = \frac{1}{\exp(\epsilon_i - \epsilon_F - eE\vec{r}_i - \mu_i) + 1} \tag{2.21}$$

First, note that in the case of $\epsilon_i = C$ for all i, i.e. no disorder in the energy levels, we find:

$$\mu_i = -e\vec{E} \cdot \vec{r_i} \tag{2.22}$$

So, we see that electrons move in the direction of decreasing potential, as we would expect. Furthermore, note that increasing p_i implies increasing μ_i. This is what we would expect: if the field causes an increase in the chance of being occupied for a certain site, electrons will have more difficulty entering it because no site can be doubly occupied; this translates into a higher potential for that site.
This can be made clearer by considering the form of the electrochemical potential in first order(in the electric field):

$$\mu_i(E) = \frac{kT(p_i(E) - p_i(0))}{p_i(0)(1 - p_i(0))} - eE\vec{r}_i + \mathcal{O}(E^2) \tag{2.23}$$

where we treat p_i and μ_i as functions of the electric field E. Note that low-field fluctuations of occupation probability are linearly related to those of the potential.
Finally, to make the definition clearer, consider figures 2.1 and 2.2. They show the electrochemical potential in the low-field limit for a two-dimensional sample with no energy disorder, but with some impenetrable barriers. Note in the second case that between the barriers the electrons have no choice but to move against the field, so the potential decreases from right to left there.

2.7 Single-carrier devices

To make comparison with experimental results possible it is important to translate mobility calculations into a $J - V$ characteristic for a device, with J the current density and V the applied voltage. Consider a polymer layer of thickness L sandwiched between two electrodes. Using the definition of the mobility, ignoring diffusion, and assuming the current is space charge limited, we have:

$$\begin{aligned} &J = n(x)E(x)q\mu(T, n(x), E(x)) \text{ for all } x \text{ with } 0 \leq x \leq L \\ &\tfrac{\mathrm{d}E}{\mathrm{d}x} = \tfrac{en(x)}{\epsilon_0\epsilon_r} \\ &V = \textstyle\int_0^L E(x)\mathrm{d}x \end{aligned} \tag{2.24}$$

with x the distance from the injecting electrode, ϵ_0 the vacuum permeability and ϵ_r the relative dielectric constant of the polymer. We take $\epsilon_r = 3$, a typical value for these polymers[7].
A problem with solving these equations is that the spread in site energies σ, the distance between sites R_0 and the tunnelling rate ν_0 are generally not known for specific polymers. They will be chosen to obtain the best overall fit.
One final note: in the single-carrier devices we consider the carriers are generally holes, not electrons. However, this has no consequences except for some sign changes.

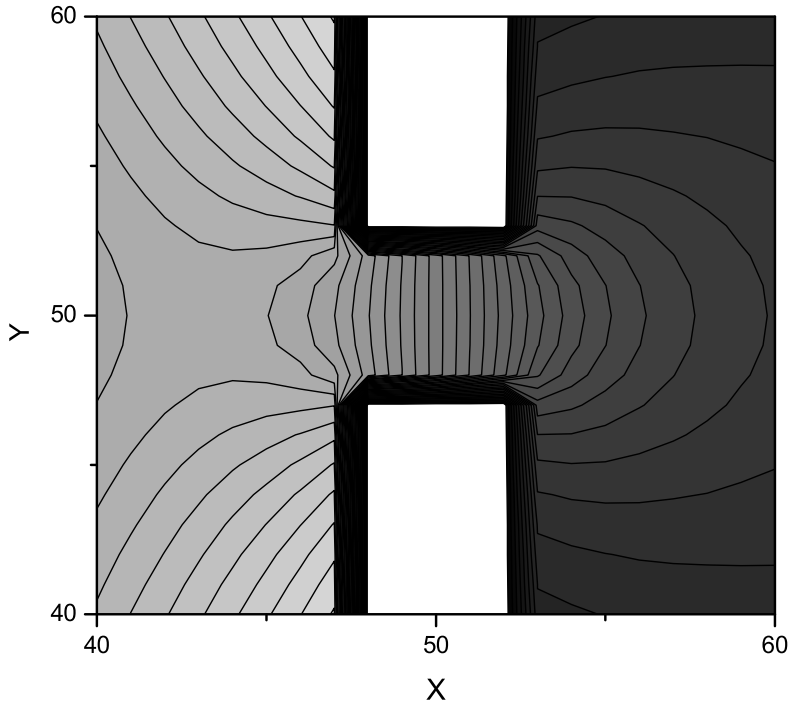

Figure 2.1: Electrochemical potential in the low-field limit for a two-dimensional sample without energy disorder and with some impenetrable barriers(represented by white rectangles). The field is in the $+X$ direction. Only a part of the sample is shown(namely with X from 40 to 60 out of 100 and the same for Y). The dimensionless inverse localization length is 20, the density 0.1 and the inverse temperature 4.

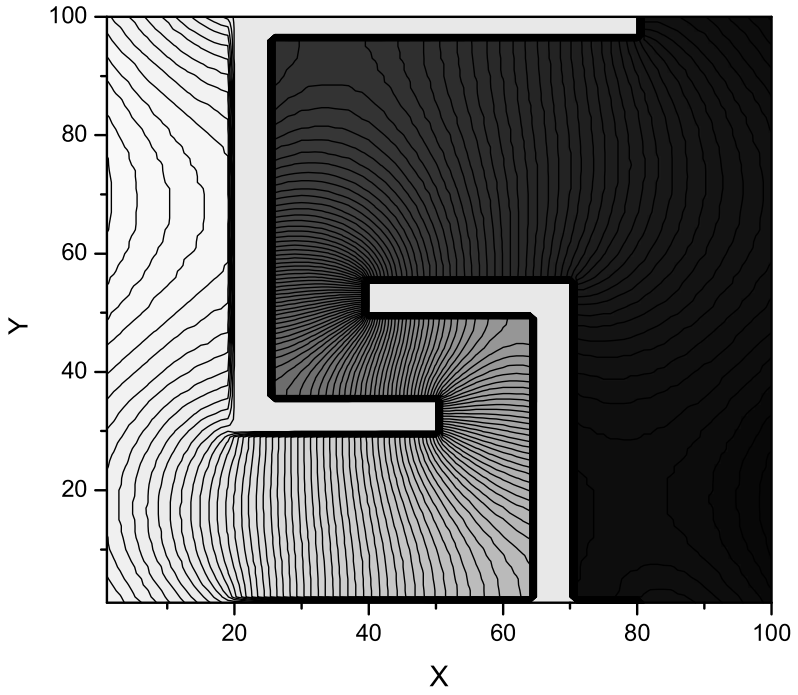

Figure 2.2: Electrochemical potential in the low-field limit for a two-dimensional sample without energy disorder and with some impenetrable barriers(represented by white rectangles). The field is in the $+X$ direction. The dimensionless inverse localization length is 20 ,the density 0.1 and the inverse temperature 4. The same situation, but with energy disorder, is shown in figure 4.5.

Chapter 3

Implementation

3.1 Iteration scheme

3.1.1 One-site clusters

It is time to find a method to solve the Master equation 2.16:

$$\begin{aligned}&\sum_j (W_{ij} p_i (1 - p_j) - W_{ji} p_j (1 - p_i)) = 0\\ &0 \leq p_i \leq 1\\ &\sum_j p_j = nL^3\end{aligned}$$

Note that the first part of this equation can be rewritten as follows:

$$p_i = \frac{\sum_j W_{ji} p_j}{\sum_j (W_{ij}(1 - p_j) + W_{ji} p_j)} \tag{3.1}$$

Note that p_i does not occur on the right-hand side of this equation. Therefore, we can use it as an iteration scheme, by applying it to every site. Following [12], implicit iteration is used, i.e. new values for p_j are used in equation 3.1 if they have already been calculated. As initial distribution we use the Fermi distribution found in the zero-field case, as discussed in section 2.5.
Now, since all we have done is rewrite the first part of equation 2.16, it is clear that whatever our iteration scheme converges to will satisfy this part of the equation. However, we also would like it to satisfy the other two parts. It can easily be seen that if the initial distribution satisfies the second part, then so will every step of the iteration. However, finding a solution that also satisfies the third part, the density condition, is more subtle.
A very simple solution would be to let it be. We can just let the iteration converge to some distribution and accept whatever density we find. We can expect a higher density for the initial distribution to lead to a higher density in the converged distribution, so making plots of the mobility as a function of density is still possible. However, this approach has three major drawbacks.

In the first place, if we want to make a plot of the mobility as a function of some other variable, keeping density constant, we have no easy way to do this. Also, we can't calculate the mobility multiple times, for different realizations of the energy disorder, for the same density. Most importantly, even density plots won't come out right, as can be seen in figure 3.1.1.

The above method is still not impossible; we can try different values of the

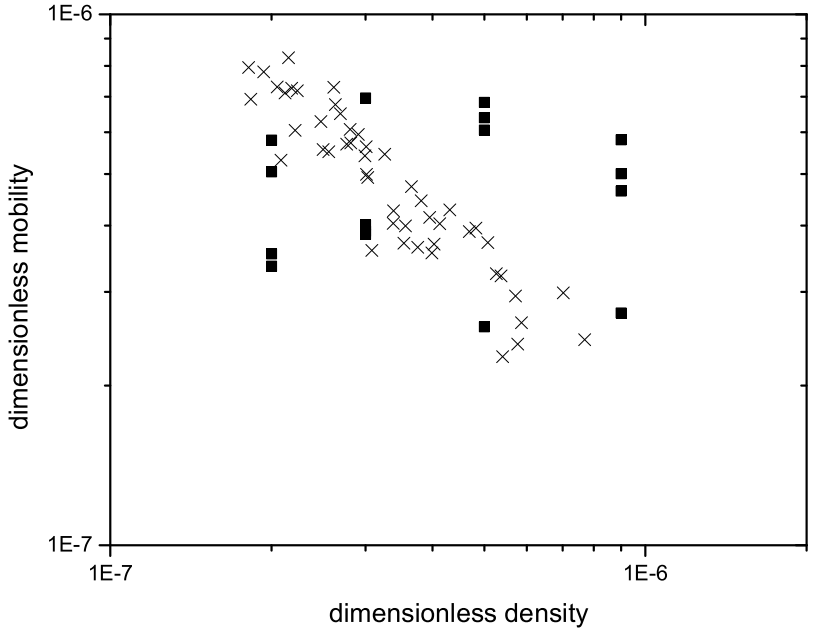

Figure 3.1: Mobility(for multiple realizations of the energy disorder), with dimensionless inverse temperature 3.6, inverse localization length 10 and field 10^{-3}. The crosses are data acquired by choosing the density in the initial distribution equal to 10^{-8}, without rescaling between iterations. The squares are data acquired by setting the density in the final distribution, by rescaling between iterations, to $2*10^{-7}$, $3*10^{-7}$, $5*10^{-7}$ and $9*10^{-7}$. We can see that there is a false density dependence visible in the crosses, showing that this method is incorrect.

initial density until we get the final density we want. However, this is very inefficient. Another option is to use an alternative iteration scheme that simulates the time evolution from the initial distribution. The density is then guaranteed to remain constant. However, the convergence speed of this method was found to be vastly inferior.

The solution is to rescale between iterations. An easy way to do this is simply multiplying every p_i by some constant factor chosen so that the desired density is found; however, this might lead to p_i's greater then 1, violating the second part of equation 2.16.
Instead, we use the electrochemical potential, as defined in equation 2.21 in section 2.6. Using the p_i resulting from the iteration up to the moment of rescaling, μ_i is calculated for every site. Then, we can find new p_i satisfying the density condition by changing the Fermi level ϵ_F and applying equation 2.21 again.

3.1.2 Two-site clusters

Just like for clusters of one site(equation 3.1), it is possible to write the probability that a cluster of two sites is in a certain state as an explicit function of the occupation probabilities of all other clusters. This can then be used as an iteration scheme as described above. The formula's are found by solving the first four parts of equation A.2 for $\alpha_{x,.}$; they are very cumbersome and completely uninteresting, and so they will not be included here. As initial distribution we use the result of one-site iteration. Only clusters of adjacent sites parallel to the field will be considered.
One important difference is that our rescaling method doesn't work here. This isn't really a problem, since we need results for two-site clusters only to compare them with those found for one-site clusters; we can simply accept whatever density we find and compute the one-site cluster mobility for that density.

3.2 Implementation details

There are some issues left to be addressed. In the first place, we need a way to know when to stop iterating. Since we are only interested in the mobility, not the distribution itself, we can calculate it every n iterations and estimate the relative error, assuming approximately exponential convergence:

$$\text{err} = \left| 1 - \frac{\mu_i - \mu_{i-n}}{\mu_{i-n} - \mu_{i-2n}} \right|^{-1} \tag{3.2}$$

Here, μ_i is the mobility after i iterations, not to be confused with the electrochemical potential at site i. This formula is only valid if $|\mu_i - \mu_{i-n}| \leq |\mu_{i-n} - \mu_{i-2n}|$; otherwise we are not yet converging exponentially and we don't stop iterating.
Typically, n is taken around 30, and a relative error of 10% is tolerated. This may seem like a high error, but generally the mobility runs through several orders of magnitude for the ranges of input parameters we consider, so this is acceptable.
Of course, equation 3.2 may be satisfied by accident long before convergence is achieved, so we require that it is satisfied a number(typically 3) of times in a row.
Once convergence has been achieved, we check whether the charge density is

within a certain margin of the desired density(typically a relative error of 10^{-4} is tolerated). If not, we rescale as described in section 3.1.1, and wait for convergence again. This is repeated as often as necessary.
Note that for typical sample sizes(100x100x100) evaluating equation 3.1 for all i would take a very long time(of the order of L^6, 10^{12} in this case). This is why we only consider jumps from sites to sites within a cubic so-called springbox around it. Typically, this cube is 3 or 5 sites in length. This length is chosen so that increasing it does not significantly influence the mobility.
Note that there is a random element in that the energy levels of the sites are normally distributed. Of course, if we take the sample size to infinity as we should, this will not be a problem as the spread in the mobility will go to 0. However, due to memory constraints, taking a very high sample size(above 150x150x150) is impossible. This means we have to do multiple runs, for different realizations of the energy disorder. Typically, we do between 10 and 50 runs, stopping when the estimated standard deviance is smaller than 10%.
It is important to note that this doesn't completely simulate taking the limit of infinite sample size, so it is necessary to take the sample size large enough, so that increasing it doesn't change the average mobility found. Typically this requires a sample size so that there are at least a few electrons present(i.e. nL^3 should be of the order of at least unity), especially for low temperatures.
One final note: for all calculations the one-site approximation is used. The two-site equations are used only to check the validity of this approximation.

Chapter 4

Results

4.1 Field dependence of the mobility

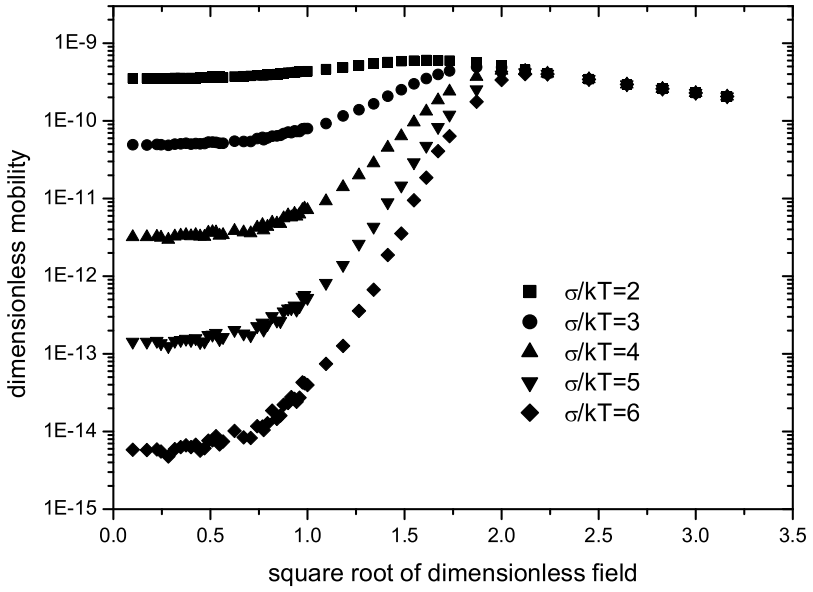

Figure 4.1: Mobility as function of field, with dimensionless inverse localization length 20, density 10^{-6} and various temperatures as shown.

Field dependence results for different densities and temperatures are shown

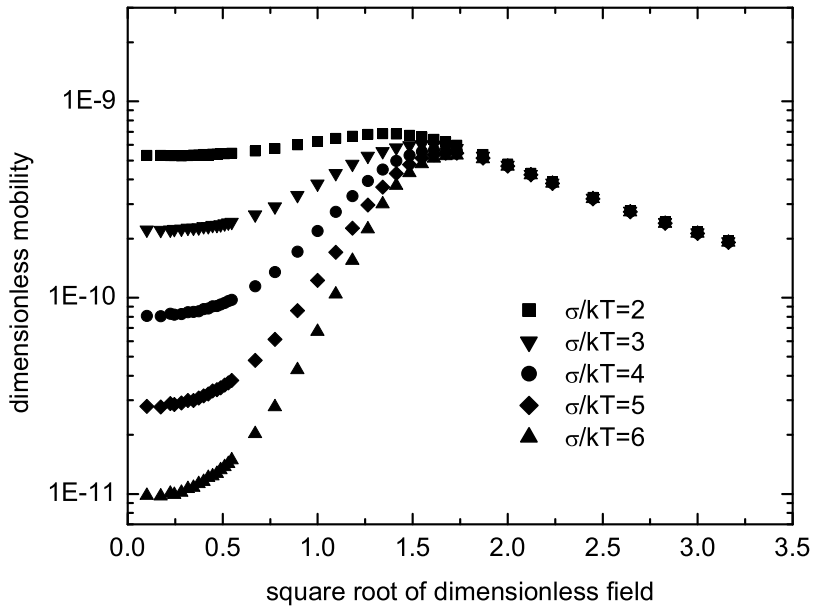

Figure 4.2: Mobility as function of field, with dimensionless inverse localization length 20, density $5 * 10^{-2}$ and various temperatures as shown.

in figures 4.1 and 4.1. Some characteristics of these dependencies can be derived.
First, let's consider what happens in the low field limit. Since the only orientation in our model is the direction of the field, reversing it should not change the mobility. The mobility is therefore an even function of the electric field, and assuming it is analytic its derivative must be zero at zero field. This can clearly be seen in the results.
There is more to be said about this limit. We can assume that in the low field limit the occupation probabilities of the sites p_i change linearly with the field. This can be used to rewrite equation 2.16 into a set of linear equations. These can then be solved using standard techniques, yielding the mobility in the low field limit. This approach will not be used here however.
The behavior of the mobility in the high field limit is also easily derived. After all, in this case it becomes virtually impossible for an electron to jump against the field, and all jumps in the direction of the field have the same rate, since in the case of a lower energy for the destination site the jump rate does not depend on the energy difference(equation 2.1). Since all sites are equal now, we have $p_i = n$. Using equation 2.19 then yields, using dimensionless parame-

ters(equation 2.2):

$$\frac{\mu\sigma}{R_0^2\nu_0 e} = \frac{\exp(-\alpha R_0)(1-n)}{eER_0/\sigma} \tag{4.1}$$

4.2 Density and temperature dependence of the mobility

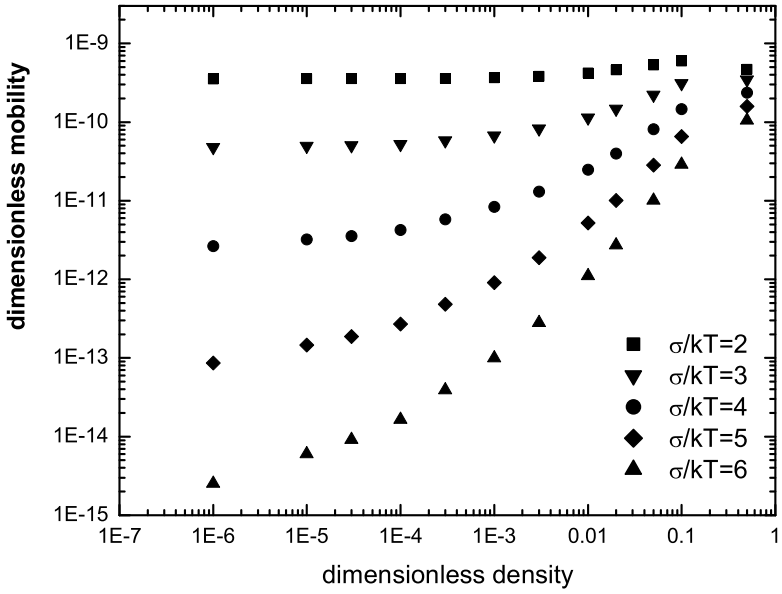

Figure 4.3: Mobility as function of density, with dimensionless inverse localization length 20, field 10^{-3} and various temperatures as shown.

Density dependence results for different temperatures are shown in figure 4.2. Again, some of its characteristics can be explained.
First, notice the existence of the low density limit(not visible for all temperatures). This can easily be understood; after all, at some point the interaction between electrons(due to Fermi exclusion) becomes negligible. Mathematically, we exclude all terms that are second order in the occupation probabilities, i.e. terms of the form $p_i p_j$. Equation 2.16 then becomes:

$$\begin{aligned} \sum_j (W_{ij} p_i - W_{ji} p_j) &= 0 \\ \sum_j p_j &= nL^3 \end{aligned} \tag{4.2}$$

Note that the condition $0 \leq p_i \leq 1$ has been removed, since there is only one solution to equation 4.2 anyway, and it should satisfy this condition automatically in the low density limit.
Now, suppose we have a solution p_i to equation 4.2 for some density n_1. Write this as $p_i(n_1)$. It can easily be checked that:

$$p_i(n_2) = \frac{n_2}{n_1} p_i(n_1) \tag{4.3}$$

Calculating the mobility, again excluding second order terms, now yields:

$$\mu(n_2) = \frac{\sum_{i,j} W_{ij} p_i(n_2)(\vec{r}_j - \vec{r}_i) \cdot \hat{E}}{n_2 L^3 |\vec{E}|} = \frac{\sum_{i,j} W_{ij} \frac{n_2}{n_1} p_i(n_1)(\vec{r}_j - \vec{r}_i) \cdot \hat{E}}{n_2 L^3 |\vec{E}|} = \mu(n_1) \tag{4.4}$$

Next, note that the mobility increases with increasing density(up to 0.5). To

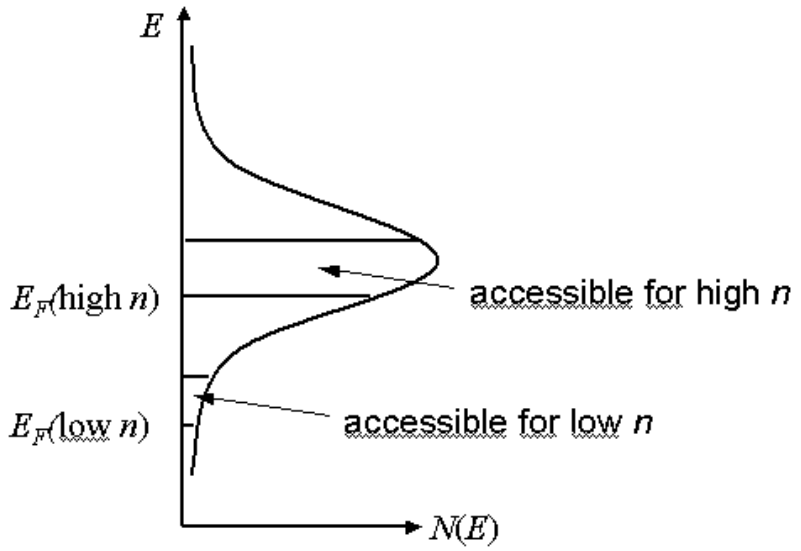

Figure 4.4: Density of states, with Fermi levels and hopping ranges for both low and high densities.

understand this, consider figure 4.2. This shows the approximate occupation probability in the density of states. Note that large jumps up in energy will hardly occur(equation 2.1), so significant hopping will only occur near the Fermi level. Therefore, the mobility depends strongly on the density of states at the Fermi level, which increases with increasing density.

Finally, the density increases with increasing temperature, as can be seen in

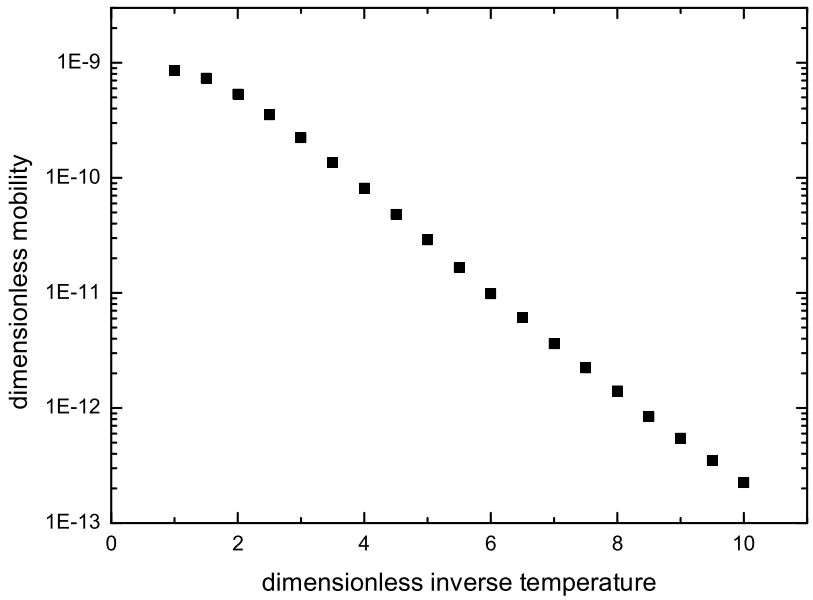

Figure 4.5: Mobility as function of temperature, with dimensionless tunneling rate 20, field 10^{-3} and density $5 * 10^{-2}$.

more detail in figure 4.2. This can be understood using figure 4.2 as well. After all, a high temperature means that jumps with a greater energy difference become feasible, and the band in which hopping can occur becomes wider.

4.3 Effects of using one-site clusters

For the above results one-site clusters were used. To determine the validity of this mean-field approximation, we compare the results with those using two-site clusters. Unfortunately due to computation limitations only (reasonably) high temperatures can be considered. By analyzing the trends we can still validate the mean-field approximation however, except for very low temperatures and high densities.
First, a word on how these results were obtained. The accuracy demanded in convergence was raised from 10% for the values above to 10^{-5}. This was necessary to consistently observe the small differences in mobilities between the one-site and two-site cluster methods. These differences are also smaller than

the spread in mobilities for different instances of the energy disorder, but luckily the difference itself exhibited a much smaller spread.
The results themselves can be seen in figures 4.3, 4.3 and 4.3. We see that the mobility for two-site clusters is lower than that for one-site clusters, and that the difference is small, typically around 0.02. Also, the difference increases with decreasing temperature and decreases with decreasing density. Based on the trends observed it seems that the mean-field approximation will only fail significantly if the temperature is very low and the density quite high, around 0.1.
That the difference in mobilities decreases with decreasing density can be quite easily understood. After all, the difference is due to correlation effects between sites. Since these effects come into play when two electrons are on neighboring sites, they scale with n^2 and will quickly become negligible for low n.

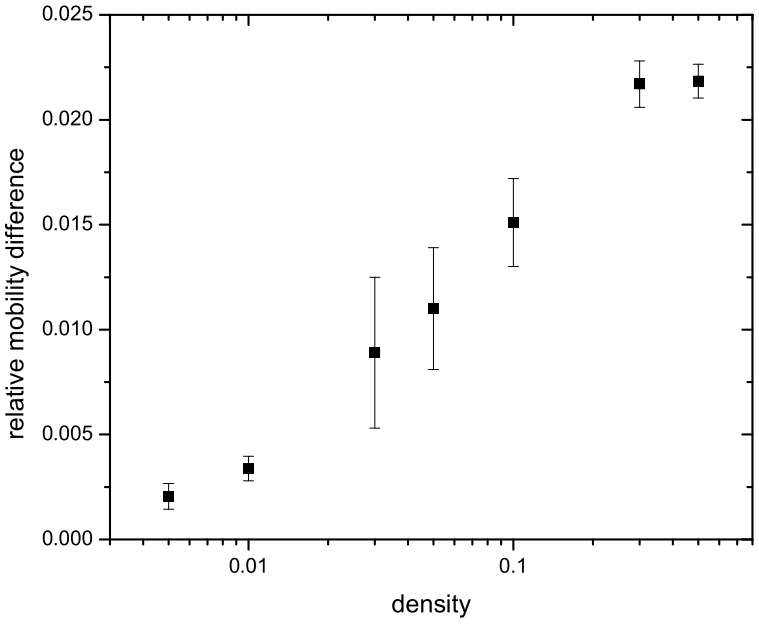

Figure 4.6: Relative difference between one-site and two-site cluster mobility (the two-site cluster mobility is always lower) as a function of carrier density. The dimensionless field is 0.01, the inverse temperature 2 and the inverse localization length 20. Note that the relative difference decreases with decreasing density. The sudden drop in error at a density of 0.01 is because larger samples were used here.

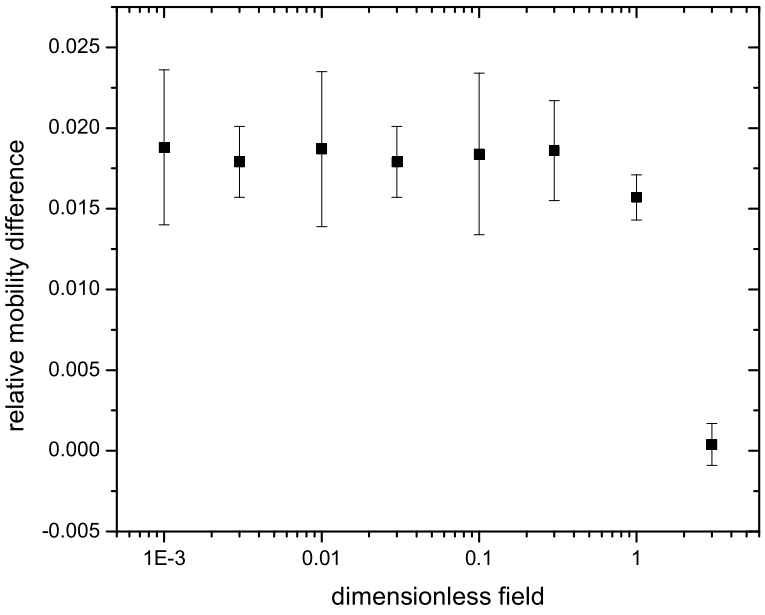

Figure 4.7: Relative difference between one-site and two-site cluster mobility (the two-site cluster mobility is always lower) as a function of field. The dimensionless density is 0.05, the inverse temperature 3 and the inverse localization length 20. No field dependence is visible until the high field limit described in section 4.1 is reached.

4.4 Using the Fermi distribution instead of solving the Master equation

As noted in section 2.5 we can ignore the Master equation altogether and simply use the Fermi distribution to calculate the mobility. Results for this method are compared with those found by solving the Master equation in figure 4.4. It can clearly be seen here that this approximation is too crude, unfortunately invalidating the results found in [11].

4.5 Graphs of the electrochemical potential

Let's have a look at what the distribution of charge carriers looks like, using the electrochemical potential described in section 2.6. Results can be found in

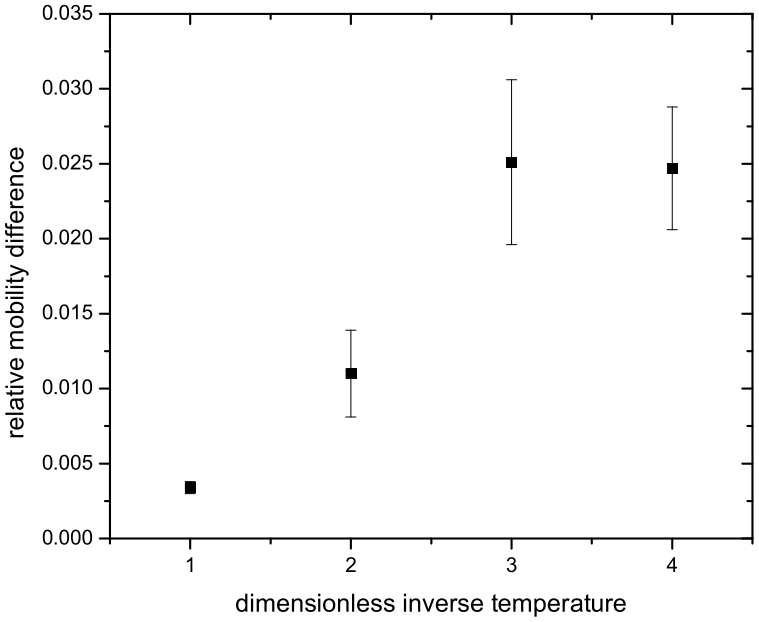

Figure 4.8: Relative difference between one-site and two-site cluster mobility (the two-site cluster mobility is always lower) as a function of inverse temperature. The dimensionless density is 0.05, the field 0.01 and the inverse localization length 20. Note that the relative difference increases with decreasing temperature.

figures 4.5 and 4.5 for high and low temperatures respectively. Also, the effect of energy disorder in a system with impenetrable barriers is shown in figure 4.5. Note that the potential landscape is characterized by plateaus of reasonably constant potential, followed by cliffs where the potential drops off steeply. This is caused by charge carriers lining up for a difficult jump. This also explains why the effect is much smaller at higher temperatures: difficult jumps are much less pronounced due to the exponential form of the jump rates(equation 2.1).

4.6 Results for single-carrier devices

The solution of the single-carrier device equation 2.24 for two polymers is compared with experimental results in figure 4.6. The theoretical results were calculated by Frank Pasveer and Peter Bobbert. Fitted values for σ, R_0 and ν_0

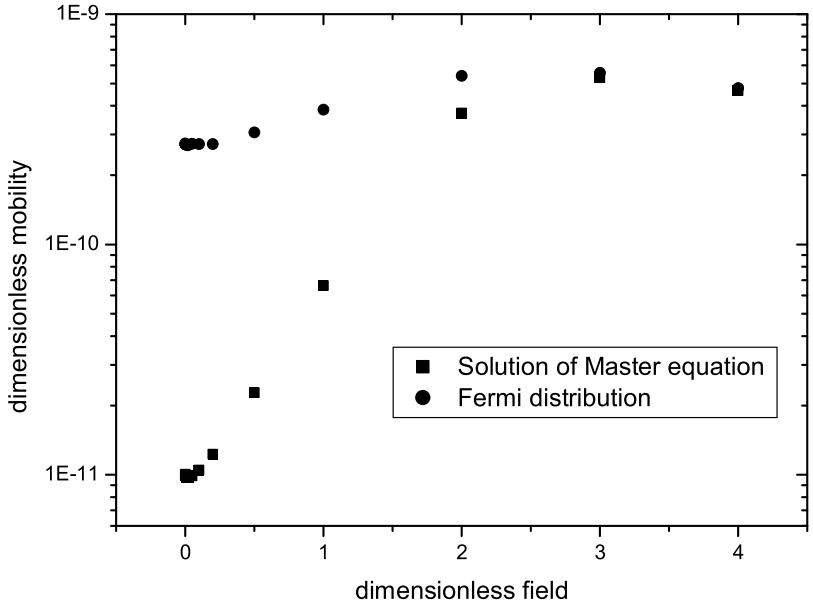

Figure 4.9: Mobility as function of temperature, with dimensionless inverse localization length 20, inverse temperature 6 and density $5 * 10^{-2}$. Results are shown both for using the solution of the Master equation and using the Fermi distribution for zero field. Note that the latter vastly overestimates the mobility.

are shown in table 4.6. Note that R_0 should be seen as an approximation, since the actual lattice is not cubic. From the figure it becomes clear that both the density and the field dependence play a role in determining device characteristics.

Polymer	$\sigma(eV)$	$R_0(m)$	$\nu_0(s^{-1})$
NRS-PPV	0.14 ± 0.01	1.8 ± 0.1	$(3.1 \pm 0.6) * 10^{18}$
C_1C_{10}-PPV	0.14 ± 0.01	1.6 ± 0.1	$(3.5 \pm 0.7) * 10^{20}$

Table 4.1: Fitted values for σ, R_0 and ν_0 in NRS-PPV and C_1C_{10}-PPV.

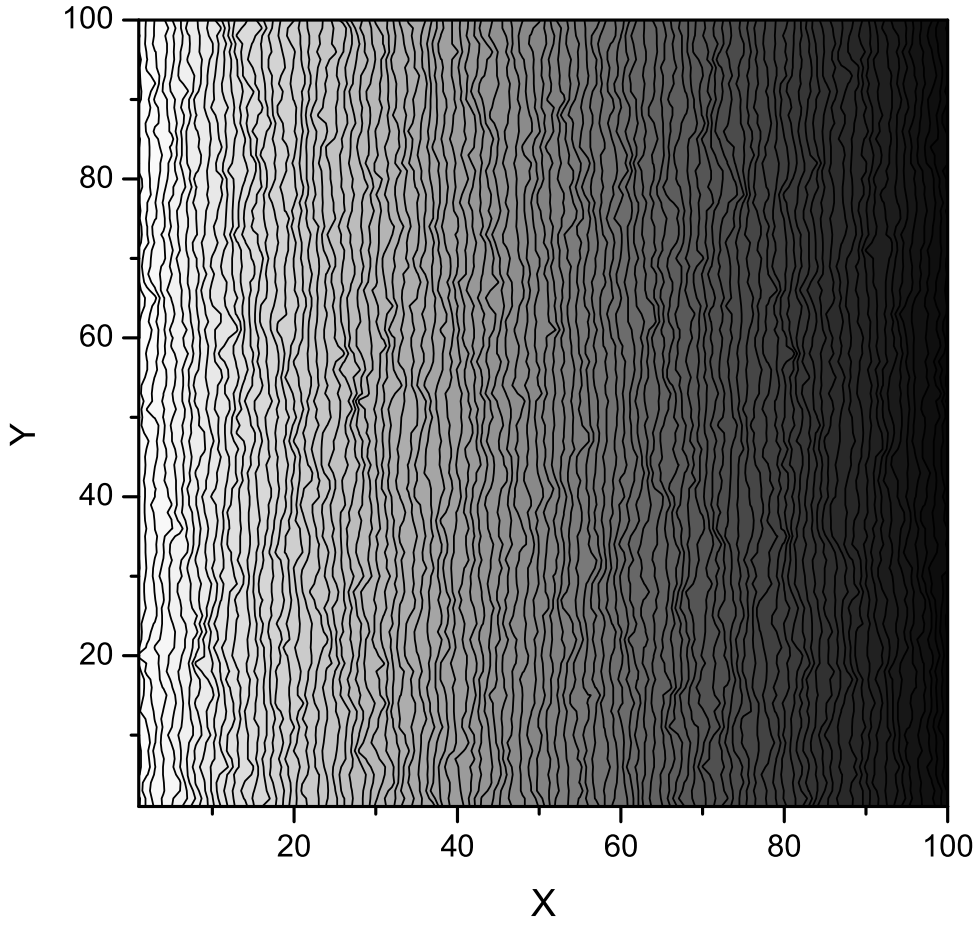

Figure 4.10: Electrochemical potential in the low-field limit for a two-dimensional sample with energy disorder. The field is in the $+X$ direction. The dimensionless inverse localization length is 20 ,the density 10^{-3} and the inverse temperature 2.

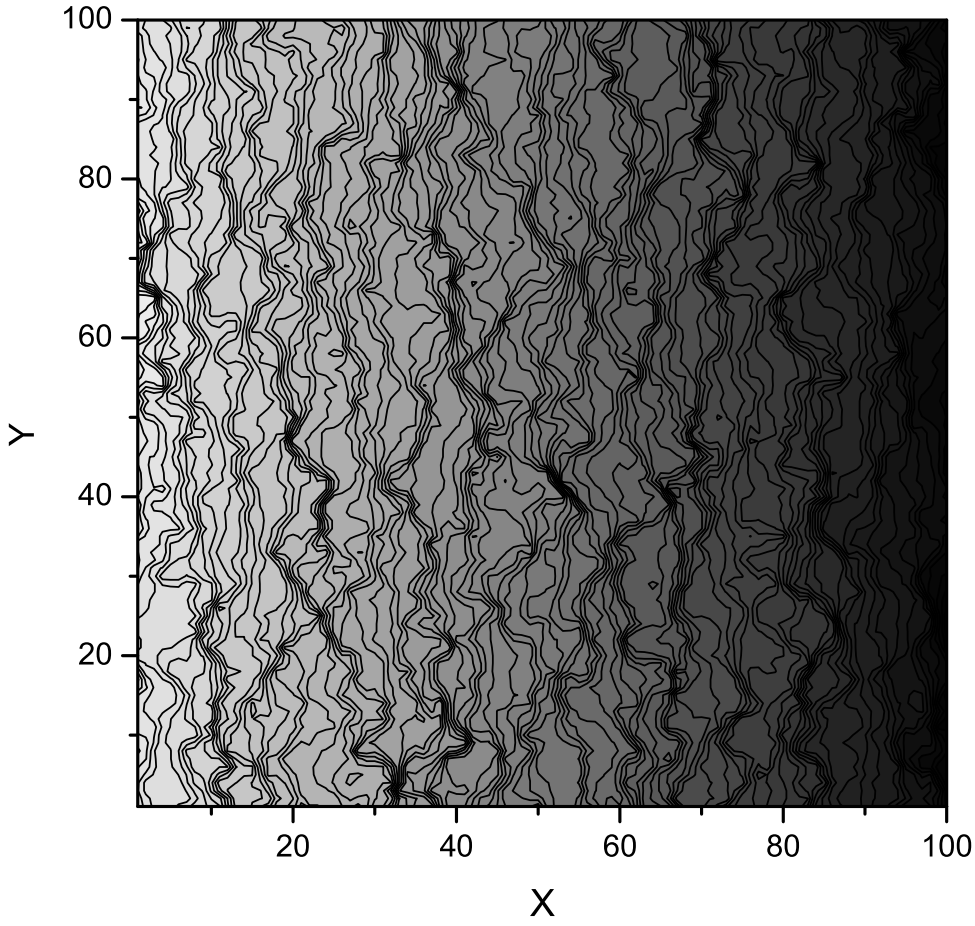

Figure 4.11: Electrochemical potential in the low-field limit for a two-dimensional sample with energy disorder. The field is in the $+X$ direction. The dimensionless inverse localization length is 20 ,the density 10^{-3} and the inverse temperature 8.

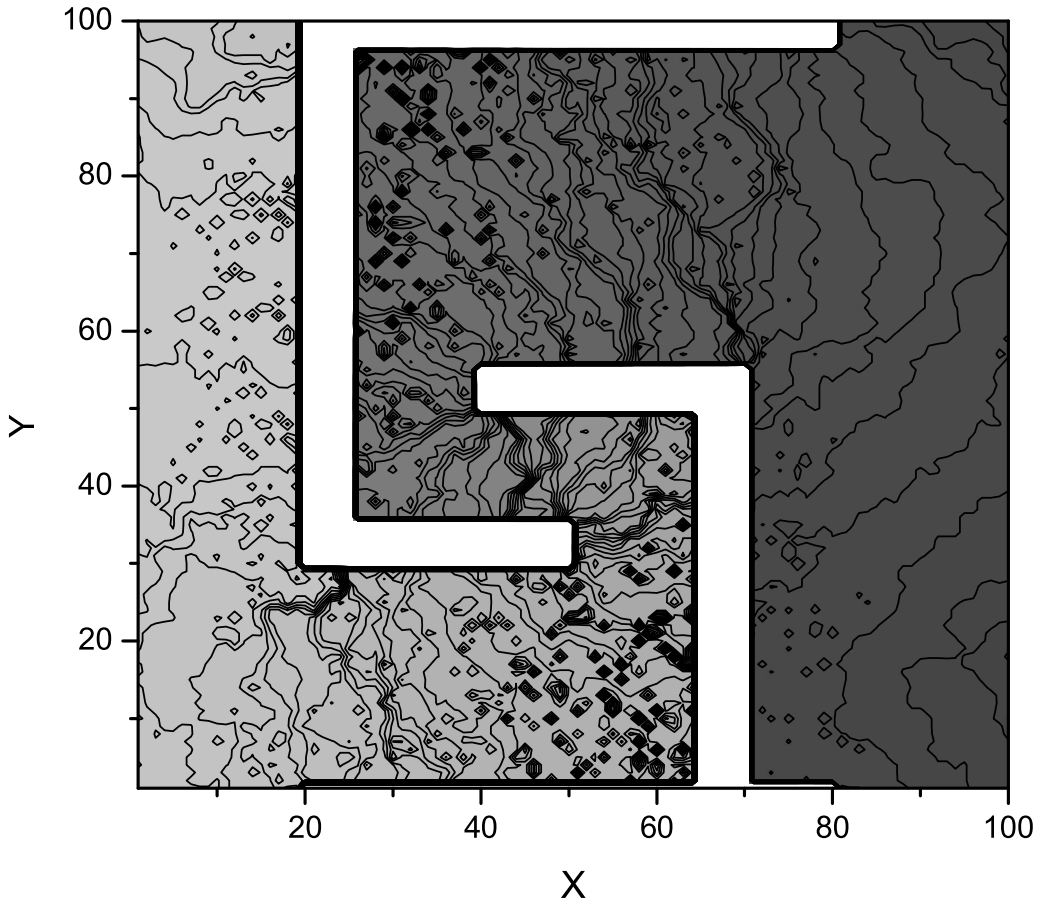

Figure 4.12: Electrochemical potential in the low-field limit for a two-dimensional sample with energy disorder and with some impenetrable barriers(represented by white rectangles). The field is in the $+X$ direction. The dimensionless inverse localization length is 20 ,the density 0.1 and the inverse temperature 4. The same situation, but without energy disorder, is shown in figure 2.2.

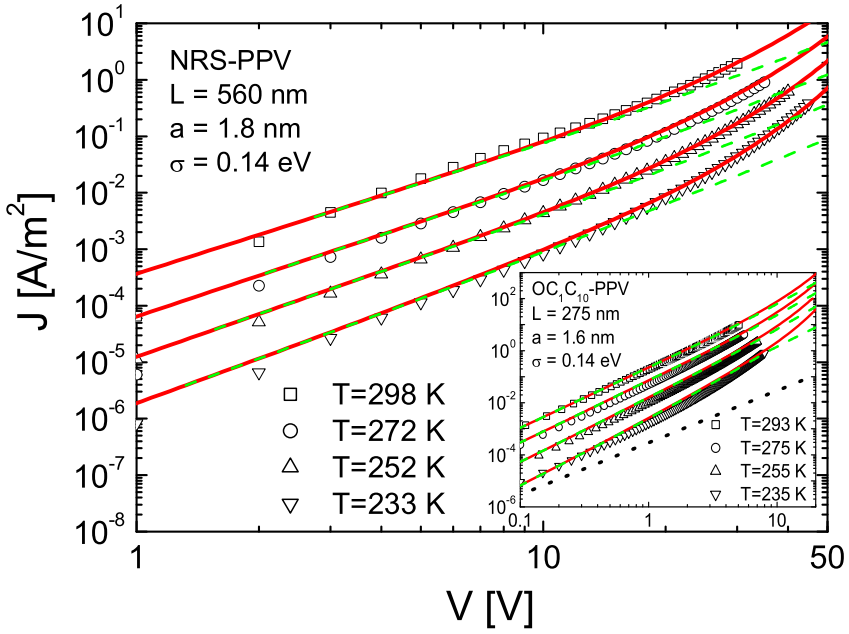

Figure 4.13: Experimental (symbols) and theoretical (lines) current-density as a function of voltage for polymer layers of NRS-PPV with thickness 560 nm (main panel) and C_1C_{10}-PPV with thickness 275 nm (inset). The full line shows the solution of equation 2.24 taking the dependency on the field and the density into account. The dashed line ignores field dependence, and the dotted line (only shown in the inset) ignores both field and density dependence.

Chapter 5

Conclusions

The first and most important conclusion is that the model described can accurately predict the dependence of the mobility on temperature, density and field. This is based on the excellent fits with experimental data. This means that our approximations are justified, like the simple Gaussian distribution of sites, the cubic lattice and the mean-field approximation. Also, there is no need to assume a correlation between site energies[12, 13, 14, 15] or multi-phonon hopping rates[16].
Our other conclusion is that it is indeed the density dependence that is mostly responsible for determining single-carrier device characteristics. The field dependence does play a role, but only at large applied voltages and low temperatures.

Bibliography

[1] A.R. Brown. C.P. Jarrett, D.M. de Leeuw, and M. Matters, Synth. Met. **88**, 37 (1997).

[2] R.H. Friend, R.W. Gymer, A.B. Holmes, J.H. Burroughes, R.N. Marks, C. Taliani, D.D.C. Bradley, D.A. Dos Santos, J.L. Brédas, M.Lögdlund, W.R. Salaneck, Nature (London) **397**, 121 (1999).

[3] L. Pautmeier, R. Richert, and H. Bässler, Synth. Met **37**, 271 (1990).

[4] H. Bässler, Phys. Stat. Sol. B **175**, 15 (1993).

[5] P.W.M. Blom, M.J.M. de Jong, and M.G. van Munster, Phys. Rev. B **55**, R656 (1997).

[6] H.C.F. Martens, P.W.M. Blom, H.F.M. Schoo, Phys. Rev. B **61**, 7489 (2000).

[7] W. F. Pasveer, J. Cottaar, C. Tanase, R. Coehoorn, P. A. Bobbert, P. W. M. Blom, D. M. de Leeuw, M. A. J. Michels, Phys. Rev. Lett. **94**, 206601 (2005)

[8] I.N. Hulea, H.B. Brom, A.J. Houtepen, D. Vanmaekelbergh, J.J. Kelly, and E.A. Meulenkamp, Phys. Rev. Lett. **93**, 166601 (2004).

[9] A. Miller and E. Abrahams, Phys. Rev. **120**, 745 (1960).

[10] T.M. Liggett, Lecture notes from School and Conference on Probablity Theory - SMR 1407, Trieste 2002

[11] Y. Roichman and N. Tessler, Synth. Met. **135**, 443 (2003).

[12] Z.G. Yu *et al.*, Phys. Rev. Lett. **84**, 721 (2000); Phys. Rev. B **63**, 85202 (2001).

[13] Y.N. Gartstein and E.M. Conwell, Chem. Phys. Lett. **245**, 351 (1995).

[14] D.H. Dunlap, P.E. Parris, and V.M. Kenkre, Phys. Rev. Lett. **77**, 542 (1996).

[15] S.V. Novikov, D.H. Dunlap, V.M. Kenkre, P.E. Parris, and A.V. Vannikov, Phys. Rev. Lett. **81**, 4472 (1998).

[16] D. Emin, Phys. Rev. Lett. **32**, 303 (1974).

Appendix A

Equations for clusters of two sites

The derivation of the balance equations for partitioning into clusters of two sites is very similar to that of 2.16, but much more cumbersome. Therefore, only the result, will be stated here. First, some notation issues. Let x be a cluster, then write x_a for the first site in x and x_b for the second. Furthermore, write o, a, b and ab for the configurations of x, with a letter showing that site occupied. So, for instance, we now have that $\alpha_{x,a}$ is the probability that x_a is occupied but x_b is not. Some further definitions:

$$\begin{aligned} p_{x_a} &= \alpha_{x,a} + \alpha_{x,ab} \\ p_{x_b} &= \alpha_{x,b} + \alpha_{x,ab} \\ ai_x &= \sum_{i \notin x} (W_{x_a i}(1 - p_i) \\ bi_x &= \sum_{i \notin x} (W_{x_b i}(1 - p_i) \\ ao_x &= \sum_{i \notin x} (W_{i x_a} p_i) \\ bo_x &= \sum_{i \notin x} (W_{i x_b} p_i) \end{aligned} \tag{A.1}$$

These can be seen as, respectively: the probabilities that site x_a or x_b is occupied, the rate of flow to site x_a or x_b if it is empty and the rate of flow from site x_a or x_b if it is occupied. Note that the rates of flow do not depend on $\alpha_{x,.}$. Writing out equations 2.10 through 2.13 now yields the equivalent of equation 2.16 for clusters of two sites:

$$
\begin{aligned}
&(ai_x + bi_x)\alpha_{x,o} = ao_x\alpha_{x,a} + bo_x\alpha_{x,b} \\
&(ao_x + bi_x + W_{x_a x_b})\alpha_{x,a} = ai_x\alpha_{x,o} + W_{x_b x_a}\alpha_{x,b} + bo_x\alpha_{x,ab} \\
&(ai_x + bo_x + W_{x_b x_a})\alpha_{x,b} = bi_x\alpha_{x,o} + W_{x_a x_b}\alpha_{x,a} + ao_x\alpha_{x,ab} \\
&\alpha_{x,o} + \alpha_{x,a} + \alpha_{x,b} + \alpha_{x,ab} = 1 \\
&0 \leq \alpha_{x,\cdot} \leq 1 \\
&\sum_{y \in X} (\alpha_{x,a} + \alpha_{x,b} + 2\alpha_{x,ab}) = nL^3
\end{aligned}
\tag{A.2}
$$

Note that these equations are linear in $\alpha_{x,\cdot}$ for fixed x, though not in $\alpha_{\cdot,\cdot}$.
The equivalent of equation 2.19, the mobility as a function of the distribution, for the case of two-site clusters is:

$$
\mu = \frac{\sum_{i,j,\{i,j\} \notin X} W_{ij} p_i (1 - p_j)(\vec{r}_j - \vec{r}_i) \cdot \hat{E} + \sum_{x \in X} (W_{x_a x_b}\alpha_{x,a} - W_{x_b x_a}\alpha_{x,b})(\vec{r}_{x_b} - \vec{r}_{x_a}) \cdot \hat{\vec{E}})}{nL^3|E|}
\tag{A.3}
$$